Leveraging Human Gait Characteristics towards Self-Sustained operation of Low-Power Mobile Devices

Vishwa Goudar, James B. Wendt and Miodrag Potkonjak
Computer Science Department
University of California, Los Angeles

Zhi Ren, Paul Brochu and Qibing Pei
Department of Materials Science and Engineering
University of California, Los Angeles

***Abstract*—The proliferation of mobile ubiquitous devices faces a hurdle in the form of high resource consumption rates that restrict longevity. Several low-power devices and application designs and optimization techniques have been proposed. Simultaneously, energy harvesting technologies are increasingly being viewed as a complementary technique to drive down resource consumption rates and even achieve self-sustenance. Towards this end, we propose a foot-strike powered harvester array composed of a novel high-energy density material called Dielectric Elastomers. To compensate for their control parameter sensitivity, we propose an adaptive closed-loop control algorithm based on general characteristics of human gait. From experimentally collected datasets of human plantar pressure and detailed characterization of DE behavior, we show that our algorithm yields enough accuracy to produce upwards of 85% of the maximum energy harvestable by the DE array. We also show that, in many cases, this is sufficient to fully drive low-power mobile ubiquitous applications.**

***Keywords*—Energy Harvesting; Mobile Devices, Self-Sustaining Devices, Dielectric Elastomer Generators**

I. Introduction

The past decade has lay witness to the manifestation of several ubiquitous mobile applications in the domains of healthcare, military, sports, entertainment and security. Fuelled by advances in low-power electronics and miniaturization, wireless standards, sensor technologies and battery power management, this proliferation of mobile-centric ubiquitous computing has contributed substantially to the social media revolution, increased productivity, improved communication and our overall quality-of-life. Sensor integrated smartphone prototypes, as well as those involving mobile peripheral or standalone devices equipped with arrays of sensors, have pushed on to yield a variety of potentially transformative applications.

Yet, resource consumption rates remain a primary concern for device portability, longevity, and ultimately for adoption rates. Driving a plethora of sensors and the related communication requires a lot of power, while battery energy densities continue to improve marginally [1]. As a result, several effective solutions have been proposed to lower energy consumption rates towards small batteries and/or longer lifetimes. Furthermore, as novel low-power designs at the component and system levels are proposed and standardized, major obstacles to ubiquitous computing continue to be eroded. As a result, the levels of energy currently achievable via complementary energy harvesting techniques are becoming enticing enough to make self-sustained operation an achievable goal. However, in the context of mobile applications, although ambient energy harvesting has been explored as a means to driving the platforms, challenges remain both in terms of usability, and the quantity and rate of energy production.

In this paper we introduce novel harvesting technique to alleviate these challenges and help bridge the gap to self-sustained performance in the context of mobile wearable devices. The underlying harvester technology for the proposed system is Dielectric Elastomers (DEs), a promising new class of high energy-density rubber-like materials that possess the ability to behave as energy generators, actuators and sensors. However, owing to its material properties and the fact that it is an electrostatic transducer, DE performance is very sensitive to its control parameters. Further complicating control, is the fact that its material properties, and consequently its transduction transfer function, is non-linear. Yet, its promise of a substantial increase in energy yield combined with its unobtrusive flexible behavior, makes it a great candidate for parasitic human energy scavenging.

Specifically, given that foot strikes are capable of producing large amounts of energy [1], we propose that this emerging class of harvesters be used to scavenges the energy expended during foot strikes, so as to power ubiquitous applications that involve human locomotion. To maximize energy throughput we present a novel closed loop control scheme that enlists the user's gait characteristics to adaptively fine tune the harvester's control parameters, thereby maximizing the net energy output. Since the non-linear nature of the transfer function makes real-time parameter estimation infeasible, we apply statistical techniques to relate a user's gait characteristics to DE transduction output, thereby enabling maximal energy output in a statistical sense, while achieving it in a computationally feasible manner. We validate our algorithms based on experimentally collected datasets of the force generated by foot strikes of multiple subjects, as well as an experimental characterization of DE behavior for the proposed transducer configuration. Our evaluation shows that a number of target applications may achieve self-sustained operation based on our proposed techniques.

II. Related Work

In the wearable systems and body area networks community, it is generally agreed upon that energy harvesting poses an important challenge and opportunity for self-sustenance.

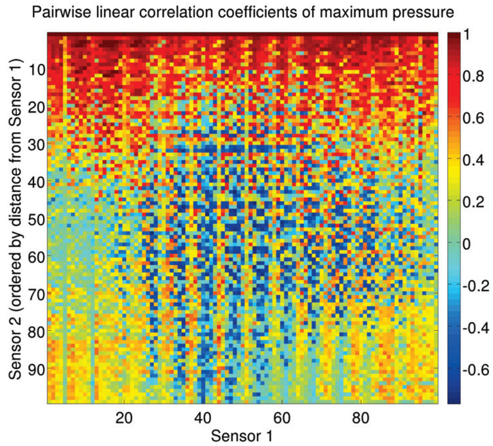

Fig. 1: Linear correlation coefficients between the maximum pressures observed at each pair of sensors.

Proposed human-powered transduction alternatives span heat transfer from the skin, vibration from foot strikes, movement of knee joints, inertia from backpacks and change in blood pressure. A wide array of human motion has been found suitable for exploitation including cranking, shaking, pushing, pumping, pulling as well as the isometric forces of squeezing and pushing [1], [2]. However, human gait offers easy pickings as the most innocuous source of human power for transduction, resulting in a long trail of harvesting designs and related patents going back to the mid 1920's [3]. The authors of [3] describe two large piezoelectric transduction elements which, when embedded into the shoe sole, is capable of producing 10mW of output and are inconspicuous to the wearer. A shoe integrated piezoelectric transducer with hydraulic-amplified input is also highlighted, which produced up to 675mW while adding significant heft to the shoe, making it unsuitable from the perspective of adoptability.

DEs are a relatively new entrant to the class of miniaturized generators. An excellent survey of the material properties relevant to its transduction mechanism, various proposed transducer configurations, capabilities in comparison to other common transducers, recent applications as well as operational boundaries and lifetime issues are detailed in [4]. We note that DEs require charging at high voltage so they may achieve their output potential; However self-priming circuits have been proposed that use an inverse charge pump to convert some of the DE voltage boost into charge, incrementally increasing the source voltage from 10V to the kV range [5]. Finally, adaptive control of DEs has been proposed in the context of actuation as a means to account for its non-linear properties, however to the best of our knowledge, we are the first to propose a energy-maximizing adaptive control technique for DE generators.

III. Background

A. Target Applications

Over the past decade, a number of custom multi-sensory devices have been prototyped towards low-power mobile ubiquitous computing. For example, the authors of [6] built a wearable activity recognition device with a power requirement of 43mW. Finally, a human balance monitoring system

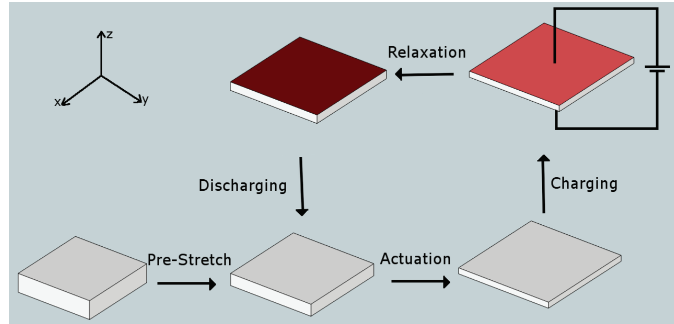

Fig. 2: Dielectric elastomer generator transduction cycle.

known as Hermes [7] was recently proposed, that measures foot plantar pressure via a multi-sensory array comprised of ninety-nine passive resistive pressure sensors. Hermes requires 183mW for operation in fully active mode and 45mW in power-efficient mode. In the latter case, the radio is assumed to transmits 25% of the time and sniff over the rest of the duration. Also, semantically driven subsampling techniques [8] are assumed to be applied, that lower the required sampling power without significantly sacrificing sensing fidelity. In lieu of the aforementioned applications, we conclude that 45mW is a suitable target required to achieve self-sustenance in the related classes of mobile ubiquitous devices.

B. Human Gait

Gait is defined as the way in which movement is achieved by humans with their limbs, such as walking, running, hopping, etc. The gait cycle, or stride, is a functional unit of gait defined as a single sequence of functions of one limb. It is divided into two phases, the stance phase, when the limb is in contact with the ground, and the swing phase, when the limb is in the air for advancement. Although gait characteristics vary across people, human locomotion, but its very nature produces commonalities across people. One such commonality is that spatial pressure profile across the sole of the foot exhibits significant local correlation. However, the amount of correlation varies with time (during a single stride) and space, contributing to the uniqueness of a subject's gait. Figure 1 illustrates the pair-wise linear correlation coefficients between the maximum pressure observed by sensors of the Hermes platform, during the stance phase of a particular subject. The sensors are organized from heel to toe on the x-axis, and for a sensor, the sensors on the y-axis are organized by their distance from it. Clearly, we observe high levels of local correlation at the top of the map. Weak correlation also exists between the heel and forefoot. It is precisely these spatial relationships that we will take advantage of to accurately predict the control parameters of the DE harvesters.

C. Dielectric Elastomer Generators

1) Material Properties: DEs are deformable yet incompressible insulating polymer films that can be built from a variety of materials. The most commonly used materials are acrylics and silicones due to their high electric permittivity (ε_r), operational boundaries, elasticity and relatively low mechanical and electrical losses. As described in [4], their relatively high elastic energy density (ranging from 5 to 40 times the energy density of piezoelectrics) means that they can store more energy when deformed, for the same amount (mass and volume) of transducer material, yielding more productive transducers. At the same time, they are quite soft compared to piezoelectrics, making them less intrusive and more comfortable to users. With electric permittivity and resistivity, DEs make for remarkable variable capacitors.

2) Transduction Mechanism: When operating in generator mode, electrical charge must be added to the elastomer surface when it is stretched. On release of the mechanical pressure, the elastic forces in the DE relax and are converted into electrostatic force. This may be conceptualized as an increase in electrical energy in the film when it relaxes, as like charges on the same surface are brought close together, and opposite charges are drawn apart. The conversion continues until the material completely relaxes, or, the increased electrostatic forces are able to maintain the film in a stretched state, albeit at a lower stretch. This transduction cycle is expressed diagrammatically in Figure 2.

If the length and width of the elastomer film each increase by a factor of λ when stretched, the area will have increased by a factor of λ^2. As an incompressible material, the volume must stay constant to cause a decrease in thickness by a factor of λ^2, leading to an increase in capacitance by a factor of λ^4 (equation (1b)). The reason behind the high energy density of DEs is underscored by equations (1b) thru (1d), where Q, V, and ΔE_{DE} are the applied charge, applied voltage and net energy output of the DE, respectively. If it fully relaxes, the electrical energy in the film will have increased to a factor of λ^4 of the input electrical energy. This is in contrast to a maximum λ^2 factor increase in energy in conventional electrostatic transducers, a limitation of their rigid structure.

$$C_\lambda = \frac{\varepsilon_0 \varepsilon_r \lambda^2 A}{\frac{d}{\lambda^2}} \tag{1a}$$

$$= \lambda^4 C_0 \tag{1b}$$

$$\Delta E_{DE} = \frac{Q^2}{2C_0}\left(\frac{1}{\lambda^4_{final}} - \frac{1}{\lambda^4_{init}}\right) \tag{1c}$$

$$= \frac{C_{\lambda_{init}} V^2}{2}\left(\frac{\lambda^4_{init}}{\lambda^4_{final}} - 1\right) \tag{1d}$$

IV. Transducer Configuration and Transduction Model

Figure 3 shows the bulge transducer configuration that we propose for our application. It involves a thin acrylic layer, a little larger than the requisite active DE area, with a hole in its center to accommodate the active area. The DE film is pre-stretched and laminated onto the acrylic backing. Deformation in the film is brought about by a driver component that is affixed to the insole of the shoe at the targeted DE location. This yields a bulge deformation in the DE when pressure is applied, with a proportionate reduction in material thickness. A harvester will have a circular active area, 1cm in diameter, with a DE film that is 5mm thick and prestretched to 400% by 400%. The harvesters are made of the 3M manufactured VBH4905 acrylic DE, the material properties for which are available in [9].

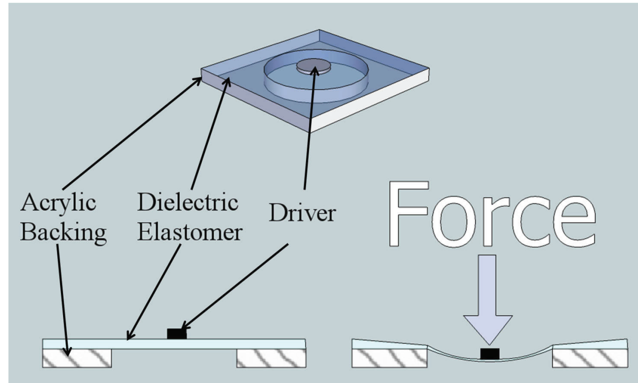

Fig. 3: Proposed DE transducer configuration.

To compute the net output energy of such a transducer, we modeled its stress-stretch behavior based on the direct transduction bulge-configuration, and its relaxation behavior, while charged, based on the detailed transduction model outlined in [10], modified to suite the bulge configuration. Also, DEs exhibit a non-linear relationship between the applied pressure and the resulting deformation; Therefore, we experimentally measured and fit this relationship, for the proposed configuration, to the Ogden hyper-elastic model.

Based on these models and our plantar pressure datasets, we determined that charging each DE in the array beyond 8kV would produce sub-optimal energy outputs owing to incomplete relaxation at the end of the transduction cycle. We further concluded that, in order to enforce operation of the DE within its mechanical operational boundaries and ensure user comfort by preventing over 6mm of compression, we would require at least 9 layers of DE film per transducer. We assume these to hold as the DE operational parameters. Finally, given that DEs can operate as sensors and generators, and that they can be charged at a low voltage with low energy requirements if pressure measurements are desired, colocatio of pressure sensors and harvesters can be trivially assumed.

A. System Design and Optimization Overview

The proposed harvester platform model is illustrated in figure 4. Equipped with a few pressure sensors to guide DE control parameter estimation, the platform is comprised of an array of DE harvesters placed at some subset of pedar mapping locations. It also includes an energy store such as a battery or a capacitor, that stores the harvested energy and powers the platform as well as the target application. Processing of the sensor samples towards DE control parameter estimation may be offloaded to the microcontroller of the target device.

Energy output is maximized if the harvesters are operated when maximum mechanical pressure is applied to them. It follows that maximum energy may be harvested during the

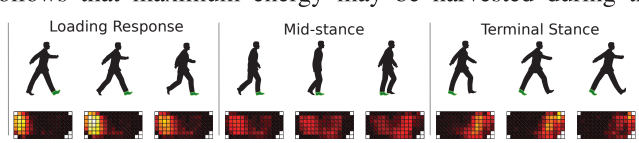

Fig. 4: Harvester Platform Model.

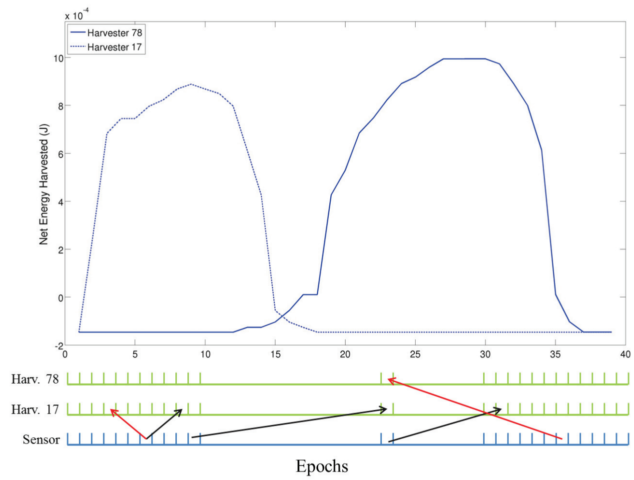

Fig. 5: Energy profiles of two harvesters with relatively large energy outputs. Valid predictions for real-time control are shown in black, while invalid ones are shown in red.

stance phase, when plantar pressure will be applied to the harvesters. Hence, we focus on this phase as the temporal domain for real-time control related sampling and energy harvesting, and assume harvester discharge to occur at the end of it.

The extent to which energy is harvested from a DE, depends on the system knowing or predicting when the maximum stretch is reached for the step (i.e. the moment the charge should be applied). Unfortunately, different users will have different stepping patterns and pressure profiles across their soles. Furthermore, ambulation timing and step pressure varies across the steps of the same user. Thus, in order to maximize the total energy collected over the DE array, the system must be able to measure and/or predict when each harvester will reach maximum stretch during a given step. Predicting these measurements requires knowledge of harvester location, pressure distribution, and step timing. Consequently, we posit that we can minimize error if this prediction is assisted, in real-time, by some pressure sampling data. The system must utilize a set of sensors measurements that are able to predict with high accuracy, the timing of maximum stretch at the harvesters.

Similarly, placement of the harvesters is not as simple as choosing the location with the highest average pressure. To achieve the final goal of maximizing aggregate net energy output from the DE array, we must consider all aspects of the individual harvesters that will contribute to their net output: (i) What is the expected energy output for the harvester; (ii) What is the expected prediction error for the harvester, and, (iii) What is the energy cost of prediction for the harvester?

Our methodology for coordinated sample selection, harvester placement and scheduling is executed in two steps. Given a training dataset, the first builds an exhaustive pool of harvester charge-timing predictors from samples at all locations on the sole and over all epochs of the stance phase. The second step calculates a subset of harvesters, while simultaneously allocating samples to predict their charge timing, in a manner that collectively maximizes the expected aggregate net harvested energy over the dataset.

Algorithm 1 Calculate AEMHPs and corresponding predictors (ILP)

Constants: $pe(s_i, h_j)$, the average harvested energy at harvester h_j based on predictions from sample s_i, C, the energy cost of each sample, and N the number of harvesters

Integer Variables: S_iH_j, an indicator for whether sample s_i will control harvesting at h_j, and S_i, an indicator for whether sample s_i will be used

Max: $\sum_{s_i}\left(\sum_{h_j}[pe(s_i,h_j).S_iH_j] - C.S_i\right)$

$\sum_{s_i} S_iH_j \le 1$ for each h_j

$\sum_{h_j} S_iH_j \le N.S_i$ for each s_i

$0 \le S_i \le 1$ for each s_i

$0 \le S_iH_j \le 1$ for each s_i and h_j

B. Predicting Harvester Energy Profiles

In order to accurately predict the optimal charge timing of the DE harvesters, we enlist the local correlation property of plantar pressure. Based on this property, an aptly placed sensor, sampling at the right, time should be able to accurately predict the timing of a number of harvesters in its neighborhood. Towards this end, we construct of a pool of robust statistical models between sensor samples and temporal profiles of harvester output. Here, we define sample $s_{i,j}$ as a single pressure measurement of the sensor i sampled at the epoch j from the start of a stance phase. Similarly, yield $h_{p,q}$ is the net energy output of harvester p after applying a charge at epoch q and discharging at the end of the stance phase. For a stride, the models corresponding to a sample may be used to predict the entire temporal profile of a harvester's output, based on the sample value. Consequently, a sample's optimal charge timing prediction would be the timing when the predicted profile achieves maximum.

Note that our goal isnt to accurately predict the temporal profile. Figure 5 illustrates the temporal profiles for 2 harvesters from a single stride by a subject. Harvester 78 sees minuscule changes in the energy scavenged between epochs 28 and 32, however, harvester 17 sees more variance around its peak output. Therefore, the quality of a predictor is not quantified by the number of epochs it is off by in predicting the instant of maximum stretch for the DE. Neither is it based on the error in its predicted value of maximum energy harvestable. Rather, the error in the predictor is defined by the difference between the amount of energy that will be scavenged, if its timing prediction is adhered to, and the actual maximum energy that can be harvested for the step. This key insight expands the solution space substantially, thereby reducing the complexity of the problem. Finally, while creating the pool of models, it is crucial that we only consider those models where the sensor sample is seen before the predicted yield, i.e. $j < q$. Obviously, hindsight is irrelevent in the context of real-time control.

In order to build a robust and effective statistical model between a valid <sample, yield> pair, we must consider, (i) the non-linearity in the relationship between samples and yields despite a high correlation in the pressure observed at the locations of the corresponding sensor and harvester, (ii)

Algorithm 2 Calculate AEMHPs and corresponding predictors (Greedy)

Input: $pe(s_i, h_j)$, the average harvested energy at harvester h_j based on predictions from sample s_i, and C, the energy cost of each sample
Output: $AEMHPr$, the AEMHP predictor set of selected samples, and $AEMHP(s_i)$, the AEMHP sets of harvesters for which s_i will be the predicting sample

$he(h_j) \leftarrow 0\ \forall\ harvesters\ h_j$
loop
  $se(s_i) \leftarrow 0\ \forall\ samples\ s_i$
  for all s_i not in $AEMHPr$ **do**
    $se(s_i) \leftarrow \sum_{h_j | pe(s_i, h_j) > he(h_j)} [pe(s_i, h_j) - he(h_j)]$ - C
    $s_k \leftarrow$ sample with maximum value in se
    if $se(s_k) \leq 0$ **then**
      Break
    else
      Add s_k to $AEMHPr$
      for all all h_j s.t. $pe(s_k, h_j) > he(h_j)$ **do**
        Remove h_j from $AEMHP(s_l)$ where s_l currently covers h_j, if $he(h_j) > 0$
        Add h_j to $AEMHP(s_k)$
        $he(h_j) \leftarrow pe(s_k, h_j)$
      end for
    end if
  end for
end loop
return $AEMHPr$ and $AEMHP$

the temporal variability inherent in the samples, and, (iii) the delay between samples and yield.

In considerations of these issues, we enlist non-parametric kernel-regression to model the <sample, yield> relationships. To account for its non-linearity, the sample value is treated as a continuous independent variable whose probability density is computed with a gaussian kernel. The sample epoch is treated as an ordered factor to explain the temporal variability in the sample, and its probability density is computed with the ordered kernel. Finally, the yield epoch accounts for the sample-yield delay, and is the other ordered factor in the model. The kernels are combined in a generalized product kernels approach, with kernel bandwidths of 2000, 0.25 and 0.25 respectively. These bandwidths were pre-determined to produce high accuracy models for our datasets. While the models are computationally expensive to produce, we note that this is done offline. The subsequent prediction required for real-time control only involves a few table lookups and few simple arithmetic operations. By repeating this prediction at each stride, our proposed control algorithm will result in charging schedules that are adaptive, depending on sensor pressure measurements, and generated in real-time. At each stride of the user, the pressure is sampled to generate a distinct harvesting schedule.

C. Aggregate Energy Maximizing Harvester Placement (AEMHP)

While we are now equipped with models that can predict the charge timing for individual DEs, it is still unclear as to which samples will drive each harvester. While we will observe local correlations, the exact spatial nature of these correlations will vary among users. Aside from this, we must also consider that some harvesters generally see insufficient input pressure and produce insignificant amounts of energy, and a few others may be too variable to predict in a manner that will result in a net positive energy output. There is also a cost involved in prediction. While each harvester can be paired up with the sample that single-handedly maximizes its expected net energy output, a better configuration may be possible if the cost of sampling is taken under advisement and multiple harvesters are predicted by a single sample, even if the individual predictions are marginally lower than the best possible sample-harvester pairings.

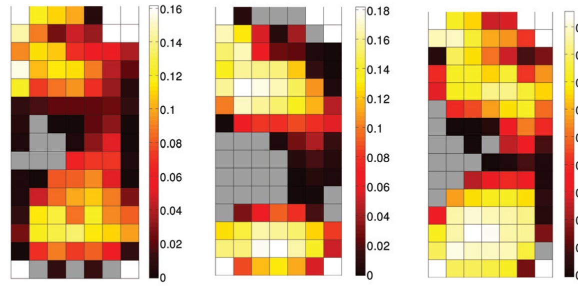

Fig. 6: Average maximum energy profiles for each of the datasets along with the output of the harvester placement algorithm. Non-selected harvesters have been grayed out. The number of samples dedicated to the real-time control of the selected harvesters are 13, 10 and 11, respectively.

With this goal of simultaneously maximizing the net energy output, we present an ILP formulation that will ensure maximum expected aggregate net energy output (algorithm 1). Due to its computationally-intensive nature, we also formulate a greedy algorithm that runs in polynomial time and produces near optimal results (algorithm 2). Judging each sample on the average net energy that it assists a harvester in producing, at each iteration the algorithm selects the sample that offers the best improvement over the covering set selected so far. In other words, a sample's merit is measured as the sum, over all harvesters, of improvements in energy harvested based on its predictions. The sample's merit is also penalized for the cost of sampling. At each iteration, the sample with the highest merit is selected into the covering set. The algorithm ends when no sample offers an improvement over the covering set selected thus far.

V. Evaluation

So we may arrive at the net energy output by the DE array for a given spatio-temporal plantar pressure profile, we experimentally characterized the stress-strain behavior of a DE harvester in the proposed transducer configuration. Next, we evaluated the system performance with experimentally collected foot plantar pressure datasets from 3 subjects. The first two datasets correspond to the gait of lighter individuals, one male and one female. The third dataset corresponds to a heavier male individual. Each of the datasets offer several steps worth of data at each of the ninety-nine pedar locations. This allows us to derive harvester performance at all harvesters and apply the proposed harvester placement, sample selection and

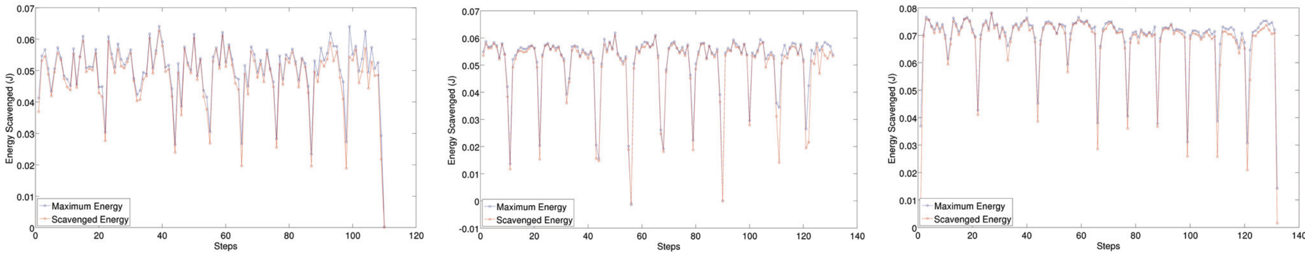

(a) (b) (c)

Fig. 7: Charts (a)-(c) refer to the maximum possible vs. achieved aggregate net energy output over all steps of each of the datasets.

real-time control algorithms, thereby evaluating the aggregate net energy output. As these algorithms involve training, we divide each dataset into a training subset comprised of 80% of the data and a testing subset comprised of 20% of the data.

VI. Results

Figure 6 presents the results of the harvester placement algorithm for each of the 3 datasets. To start off, it is clear that the users wore the system on their left foot. It also appears that user 3 is more flat-footed than the others. The figures gray out harvester that were not shortlisted into the DE array. Their locations mostly correspond to the arch of the foot where little input pressure with significant variance is seen. In most of these cases, this makes profile prediction difficult, resulting in net losses in energy output. In a few cases, the energy scavenged is too little compared to the sampling cost required to drive it. Finally, only a few samples (between 10 and 13) were required by each dataset to cover what appears to be a vast majority of harvesters in the DE array.

However, the question remains as to whether basing our decision on expected net energy output will results in large variances over the course of a walk. As we see from figure 7, little variance is seen over a majority of steps. However, some of the steps in both the training and testing datasets are a result of the subject turning around. Such steps are infrequent and provide insufficient data for the training algorithms. Due to the inadequate representation and significantly higher variance during such steps, prediction performance drops. As expected, the performance over the testing subsets (the last 20% of steps) is a bit lower compared to performance over the training subsets. On average, we observe a 10-15% energy loss over the testing subset owing mostly to prediction inaccuracies.

TABLE I: Performance Comparison of Foot Strike Energy Harvesting Systems.

Scavenger Mechanism	Net Power Output(mW)	Net Power Output Open Loop (mW)
Piezoelectric.	10	-
DE Array (User 1)	46.2	28.6
DE Array (User 2)	48.7	19.9
DE Array (User 3)	60.8	36.8

Finally, table I compares the average aggregate power output of our proposed system for each of the datasets, to a competing technologiy [1] and an open-loop control algorithm. The latter algorithm involves estimating the charge timing of each harvester as the median, over the training dataset, of the charge times when its net energy output is maximized. Owing to the superior material properties of DEs and the accuracy of our algorithm, we perform substantially well compared to the piezoelectric-driven system. Our closed-loop control-parameter estimation system also performs significantly better than the open-loop algorithm. Furthermore, the 45mW goal set for self-sustenance of low-power mobile ubiquitous devices, is observed to be achievable for each of our subjects.

References

[1] J. A. Paradiso and T. Starner, "Energy scavenging for mobile and wireless electronics," *IEEE Pervasive Computing*, vol. 4, no. 1, pp. 18–27, Jan. 2005.

[2] P. Mitcheson, E. Yeatman, G. Rao, A. Holmes, and T. Green, "Energy harvesting from human and machine motion for wireless electronic devices," *Proceedings of the IEEE*, vol. 96, no. 9, pp. 1457 –1486, sept. 2008.

[3] J. Paradiso, "Systems for human-powered mobile computing," in *Design Automation Conference, 2006 43rd ACM/IEEE*, 2006, pp. 645 –650.

[4] R. D. Kornbluh, R. Pelrine, H. Prahlad, A. Wong-Foy, B. McCoy, S. Kim, J. Eckerle, and T. Low, "From boots to buoys: promises and challenges of dielectric elastomer energy harvesting," *Polymer*, vol. 7976, no. 1, pp. 797 605–797 605–19, 2011.

[5] T. McKay, B. OBrien, E. Calius, and I. Anderson, "Self-priming dielectric elastomer generators," *Smart Materials and Structures*, vol. 19, no. 5, p. 055025, 2010.

[6] T. Choudhury, G. Borriello, S. Consolvo, D. Haehnel, B. Harrison, B. Hemingway, J. Hightower, P. Klasnja, K. Koscher, A. Lamarca, J. Lester, J. Landay, L. Legrand, A. Rahimi, A. Rea, and D. Wyatt, "The Mobile Sensing Platform: An Embedded System for Capturing and Recognizing Human Activities," *IEEE Pervasive Computing*, vol. 7, no. 2, pp. 32–41, 2008.

[7] H. Noshadi, S. Ahmadian, H. Hagopian, J. Woodbridge, F. Dabiri, N. Amini, M. Sarrafzadeh, and N. Terrafranca, "HERMES - mobile balance and instability assessment system," in *BIOSIGNALS*, 2010, pp. 264–270.

[8] J. B. Wendt and M. Potkonjak, "Medical diagnostic-based sensor selection," in *Sensors, 2011 IEEE*, oct. 2011, pp. 1507 –1510.

[9] "3M VHB$^{\text{TM}}$ tapes technical data sheet," 3M, St. Paul, MN.

[10] C. Jean-Mistral, S. Basrour, and J.-J. Chaillout, "Modelling of dielectric polymers for energy scavenging applications," *Smart Materials and Structures*, vol. 19, no. 10, p. 105006, 2010.